

Fur-regulated urease contributes to the environmental adaptation of *Yersinia pseudotuberculosis*

Junyang Wang,¹ Peishuai Fu,¹ Xinquan He,¹ Yuqi Liu,¹ Yuxin Zuo,¹ Zhiyan Wei,¹ Yao Wang,¹ Yantao Yang,¹ Changfu Li,¹ Xihui Shen,¹ Lingfang Zhu¹

AUTHOR AFFILIATION See affiliation list on p. 12.

ABSTRACT Urease converts urea into ammonia and carbon dioxide, providing a nitrogen and carbon source for microbial growth and serving as an important mechanism for human bacterial pathogens to survive in acidic conditions, which can be regulated by many factors. As a global regulator, the ferric uptake regulator (Fur) regulates a series of genes and pathways involved in many different cellular processes and the virulence of the enteric bacterium *Yersinia pseudotuberculosis* (*Yptb*). However, whether Fur regulates the urease activity in *Yptb* was still unknown. In this study, we found that urease is positively regulated by Fur in response to manganese ions (Mn^{2+}), and this regulation by Fur is mediated by specific recognition of the promoter region of urease in *Yptb*. Furthermore, urease is induced by Mn^{2+} via Fur under low nutrient conditions. Moreover, we provided evidence that urease plays an important role in acid and osmotic stress resistance, biofilm formation, and virulence of *Yptb*. Our findings provide insights into understanding the regulatory mechanism and multiple functions of urease in *Yptb*.

IMPORTANCE Urease catalyzes the breakdown of urea into ammonia and carbamate, which are widely distributed among bacterial species and play an important role as an important acid resistance system and virulence factor. In most bacterial species, urease expression is tightly regulated in response to environmental cues such as nitrogen status, pH, growth phase, substrate availability, or transcriptional regulators. In this study, we found that urease from *Yptb* is positively regulated by Fur in response to Mn^{2+} under low nutrient conditions, which functions to combat acid and osmotic stress and enhance biofilm formation, and plays a crucial role in virulence. Importantly, this is the first demonstration of a direct role for Fur and Mn^{2+} in regulating urease expression in *Yptb*. This study provides a comprehensive understanding of the regulatory mechanisms and functions of urease from *Yptb*.

KEYWORDS urease, Fur, Mn^{2+} , *Yersinia pseudotuberculosis*

Yersinia pseudotuberculosis (*Yptb*) is a Gram-negative bacterium commonly associated with foodborne illness, causing mild gastrointestinal diseases such as mesenteric lymphadenitis, appendicitis, and ileitis, as well as secondary complications such as diarrhea (1). Due to its transmission through food and water, *Yptb* often encounters acidic environments during infection, highlighting the importance of acid resistance for the survival and colonization of gastrointestinal pathogens (2). As a result, bacteria have evolved four acid resistance systems (AR1–AR4) to enhance survival (3). A functional AR3 has been reported in *Yptb*, which is crucial for bacterial survival under strong acidic conditions. Our previous study has shown that the OmpR-regulated type VI secretion system (T6SS) clusters, T6SS4, is essential for bacterial survival under acidic conditions

Editor Huaiwei Liu, Shandong University, Qingdao, China

Address correspondence to Xihui Shen, xihuishen@nwsuaf.edu.cn, or Lingfang Zhu, lingfangzhu@nwsuaf.edu.cn.

Junyang Wang, Peishuai Fu, and Xinquan He contributed equally to this article. Author order was determined by drawing straws.

The authors declare no conflict of interest.

See the funding table on p. 12.

Received 29 October 2024

Accepted 21 January 2025

Published 25 February 2025

Copyright © 2025 Wang et al. This is an open-access article distributed under the terms of the [Creative Commons Attribution 4.0 International license](https://creativecommons.org/licenses/by/4.0/).

(4). In addition, *Yptb* also uses urease to neutralize H^+ for tolerance to weakly acidic conditions by converting urea into ammonia (5).

Bacterial urease is a metalloenzyme with an active site containing nickel ions (Ni^{2+}), capable of hydrolyzing urea into ammonia (NH_3) and carbon dioxide (CO_2), increasing in environmental pH (6). The bacterial urease gene cluster consists of three main sections: structural (*ureABC*), auxiliary (*ureEFGD*), and regulatory genes (7). Notably, *ureC* is highly conserved among bacterial species, and its urease-active neutral region resides in the α -subunit, which is critical for function (8). As a crucial acid-resistance system and virulence factor, urease is prevalent in microorganisms such as *Helicobacter pylori*, *Staphylococcus aureus*, and *Yersinia enterocolitica* (9–11). Urease is responsible for acid resistance and contributes to the virulence of *Y. enterocolitica* by increasing the likelihood of bacterial survival during passage through the stomach (12, 13). However, the precise biological roles and molecular mechanisms of the urease from *Yptb* have not yet been fully elucidated.

In most bacterial species, urease expression is tightly regulated by substrate availability, growth stage, nitrogen status, pH, and even transcriptional regulators (14, 15). Our previous studies have highlighted that *Yptb* urease is regulated by various transcriptional regulators and environmental factors, including OmpR, CsrA, and RovM (2, 5). Among them, OmpR positively regulates the expression of urease, which enhances acid resistance (5), while CsrA negatively regulates the expression of urease (2). In *H. pylori*, the two-component system ArsRS, as well as a nickel response regulator NikR, sense the change in pH to activate urease expression under acidic conditions (16). A nickel-binding protein Mua represses urease expression when nickel levels are high, thus counterbalancing the NikR-mediated activation (17). In *Proteus mirabilis*, the histone-like nucleoid structuring protein H-NS has been observed to repress urease activity by repressing UreR, a urease transcriptional activator, in the absence of urea induction (18). In conclusion, it is evident that bacterial urease is subject to extensive regulation by a complex regulatory network.

Fur, known as the ferric uptake regulator, plays a crucial role in regulating iron homeostasis and metabolic pathways in bacteria (19). In many pathogenic bacteria like *Pseudomonas aeruginosa*, *Vibrio spp.*, and *Legionella pneumophila*, Fur senses a diversity of environmental stimuli and plays a crucial role in pathogenesis through regulating the expression of iron transport systems, virulence factors, and toxins in host-bacterial interactions (19). Moreover, Fur is involved in the coordination of the oxidative and acid stress defense mechanisms within the cell. *H. pylori* has a Fur-dependent two-step acid tolerance response that enhances its capacity to survive in more acidic environments (20). In *Yptb*, Fur-regulated T6SS4 and aerobactin siderophore systems contribute to oxidative stress resistance and virulence (21–23). It is noteworthy that Fur has been shown to regulate urease expression to promote bacterial survival in *H. pylori*, *Escherichia coli*, *Helicobacter hepaticus*, and *Klebsiella pneumonia* (24–28). Whether the specific link between *Yptb* urease and Fur exists is worth exploring.

In this study, we found that Fur activates urease expression by binding directly to its promoters in *Yptb* YPIII, and further studies showed that Fur-mediated expression of urease responds to Mn^{2+} under low nutrient conditions. Urease contributes to stress resistance, enhancing the survival of *Yptb* in acidic and hypertonic environments. Furthermore, urease affects the ability of *Yptb* to form biofilms and to colonize mice, thereby increasing its pathogenicity. This study provides new insights into the regulation of urease via the Mn^{2+} -dependent transcriptional regulator Fur and deepens our understanding of the regulatory mechanisms and functions of urease from *Yptb*.

RESULTS

Fur positively regulates urease expression in *Yptb*

Urease expression in *Yptb* is positively regulated by the regulator OmpR and negatively regulated by the regulators RovM and CsrA (2, 5). To determine whether Fur regulates urease in *Yptb*, we performed RNA sequencing (RNA-seq)-based transcriptomic analysis

and screened them with a threshold of $|\log_2\text{Ratio}(\Delta fur/WT)| \geq 1$. Notably, the entire urease gene cluster (Fig. 1A) showed significantly reduced transcription in the Δfur mutant compared to that in the wild type (WT) (Fig. S1). We next validated the transcriptomic data using quantitative real-time polymerase chain reaction (qRT-PCR) analysis of the *ureA*, *ureB*, *ureC*, *ureE*, *ureF*, *ureG*, and *ureD* genes in the urease gene operon. Consistent with the RNA-seq data, the expression of these genes was downregulated in the Δfur mutant (Fig. 1B). Next, we found that the expression level of urease was significantly decreased in the Δfur mutant, and this phenomenon was completely reversed in the complemented strain $\Delta fur(fur)$ (Fig. 1C). We also determined its positive regulation on urease by measuring the transcription activity of chromosomal $P_{ureABC}::lacZ$ fusions. The *ureABC* promoter activity was significantly decreased in the Δfur mutant, which could be fully restored in the complemented strain $\Delta fur(fur)$ (Fig. 1D). These data above collectively indicate that Fur positively regulates urease expression at the transcriptional level in *Yptb*.

To investigate the influence of Fur on urease production in *Yptb*, we examined the urease activity of the WT, Δfur mutant, and complemented $\Delta fur(fur)$ strains by measuring NH_3 production using the phenol-hypochlorite method as described previously (29). As shown in Fig. 1E, urease activity was significantly decreased in the Δfur mutant compared

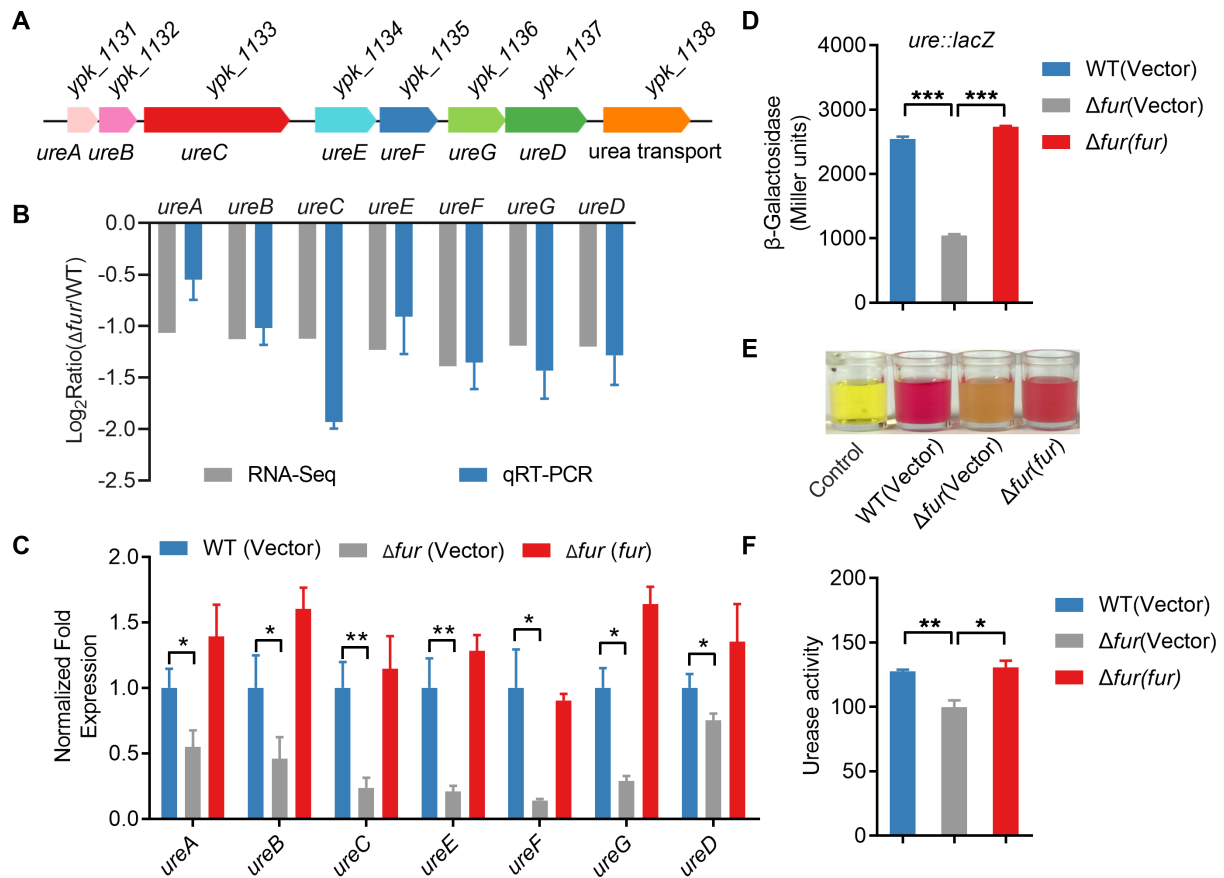


FIG 1 Fur positively regulates urease expression in *Yptb*. (A) Gene organization of urease gene cluster in *Yptb*. (B) qRT-PCR analysis of urease expression levels. Genes differentially transcribed in *Yptb* Δfur mutant compared with those in the WT were detected by transcriptomic and qRT-PCR analysis. The RNA-seq data were validated by qRT-PCR for seven urease genes (*ureA*, *ureB*, *ureC*, *ureE*, *ureF*, *ureG*, and *ureD*). (C) qRT-PCR analysis of mRNA levels of urease in *Yptb* WT, Δfur mutant, and complemented $\Delta fur(fur)$ strains. (D) β -galactosidase analysis of urease promoter activity was performed by using the transcriptional $P_{ureABC}::lacZ$ chromosomal fusion reporter expressed in indicated bacterial strains grown to stationary phase in YLB medium. (E) Qualitative analysis of urease activity for indicated bacterial strains. The pH was indicated by phenol red. (F) Quantitative analysis of urease activity for WT, Δfur , and $\Delta fur(fur)$ grown in YLB medium. Urease activity is expressed as micromoles of ammonia produced per minute per milligram of protein. Data represent the mean \pm SD of three biological replicates, each of which was performed with three technical replicates. * $P < 0.05$; ** $P < 0.01$; *** $P < 0.001$.

to that in the WT, which could be fully restored in the complemented strain $\Delta fur(fur)$. The quantitative urease activity assay further confirmed this result (Fig. 1F). Taken together, these results suggest that Fur positively regulates urease expression in *Yptb*.

Fur activates urease expression by binding directly to its promoters in *Yptb*

We have shown above that Fur positively regulates urease activity. However, the underlying mechanism is not clear. Given that Fur is a well-known regulator that regulates many iron transport systems by recognizing and binding to conserved Fur boxes within promoter regions (27, 30), we hypothesized that Fur might regulate urease by binding to its promoter. Previous studies have shown that there are three transcriptional units (*ureABC*, *ureEF*, and *ureGD*) in the urease cluster (7), with a promoter region located upstream of each unit in *Yptb* (5). We further analyzed the promoters of the urease *ureABC* operon and revealed a putative Fur-binding site at the promoter (Fig. 2A). Further analysis showed that the putative Fur-binding site is highly similar to the Fur box in *P. aeruginosa* (Fig. 2B). To further investigate the direct regulation of urease expression by Fur, we examined the interaction between Fur and the promoter of *ureABC* using electrophoretic mobility shift assay (EMSA). First, a DNA fragment of 350 bp upstream of *ureA*, designated *P_{ureABC}* was amplified and used as the probe for Fur binding. As shown in Fig. 2C, incubation of the *P_{ureABC}* probe with His₆-Fur resulted in the formation of DNA-protein complexes. Meanwhile, the specific interaction was also confirmed, as an excess of the unrelated protein bovine serum albumin (BSA) failed to form the protein-DNA complexes (Fig. 2C). Thus, we have shown that Fur activates urease expression by binding directly to its promoters in *Yptb*.

Fur-mediated expression of urease responds to Mn^{2+} under low nutrient conditions

As a key protein involved in bacterial iron homeostasis, the Fur protein plays a vital role in various metabolic regulations (31, 32). Previous studies have shown that Fur-mediated T6SS regulation is linked to Mn^{2+} levels in *Yptb* (21). Therefore, we first examined the effect of varying Fe^{3+} and Mn^{2+} concentrations on urease expression. As shown in Fig. 3A,

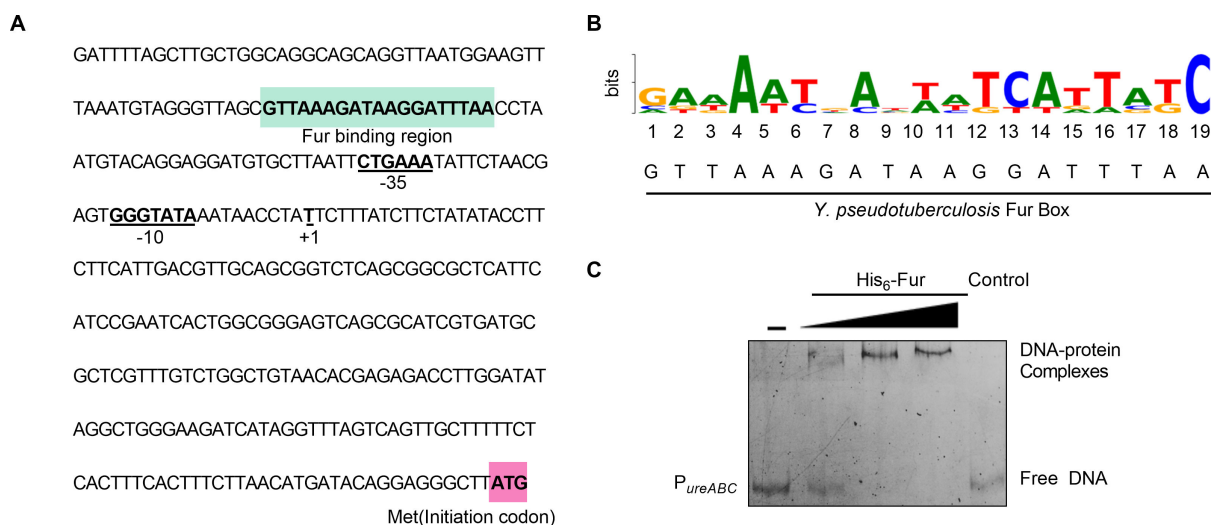


FIG 2 Fur activates urease expression by directly binding to the urease promoter in *Yptb*. (A) Identification of the Fur binding site in the promoter region of urease. Putative Fur-binding site identified in green by the online software Virtual Footprint. The ATG start codon of the first ORF of the urease is marked in pink, and the -35 and -10 elements of the urease promoter are underlined. $+1$ denotes the transcription start point. (B) Fur box sequence upstream of *ureABC*. Virtual footprint analysis of the *Yptb* Fur binding sequence. Letters represent the position weight matrix based on the *P. aeruginosa* consensus sequence for Fur binding. The Y-axis represents relative nucleotide probability, and the X-axis represents nucleotide position. *Yptb* Fur box sequence is located at -292 bp of *ureA* and has a probability score of 7.36 (max score = 9.68). (C) EMSA was performed to analyze the interaction between His₆-Fur and the urease promoter (*P_{ureABC}*). Increasing amounts of Fur (0.12, 0.34, and 1.2 μ M) and 2 ng DNA fragments were used (Control, unrelated BSA protein).

urease expression in WT was not affected by Fe^{3+} or Mn^{2+} concentration in a relatively nutrient-rich YLB medium. Remarkably, when the nutrient content of the medium was reduced by a factor of 5 ($0.2 \times \text{YLB}$), the transcriptional activity of urease increased significantly in Mn^{2+} -replete conditions rather than in Fe^{3+} -replete conditions. Furthermore, the addition of ethylenediamine-*N,N'*-bis(2-hydroxyphenylacetic acid) (EDDHA), a Mn^{2+} chelator, inhibited this increase, indicating that urease expression was unresponsive to Fe^{3+} but showed sensitivity to Mn^{2+} (Fig. 3B). To determine whether the positive regulation of urease by Fur is sensitive to Mn^{2+} concentration in *Yptb*, we determined the expression of urease in WT, Δfur , and $\Delta fur(fur)$ using chromosomal $P_{ureABC}::lacZ$ fusion reporter analysis at different Mn^{2+} concentrations. The results indicate that the presence of Mn^{2+} activates Fur-regulated urease. In the absence of Mn^{2+} , there was no significant difference in urease transcription activity between WT and Δfur mutant under $0.2 \times \text{YLB}$ conditions (Fig. 3C). Further analysis by quantitative and qualitative assessment of urease activity supported the results obtained from the β -galactosidase assay (Fig. 3D and E).

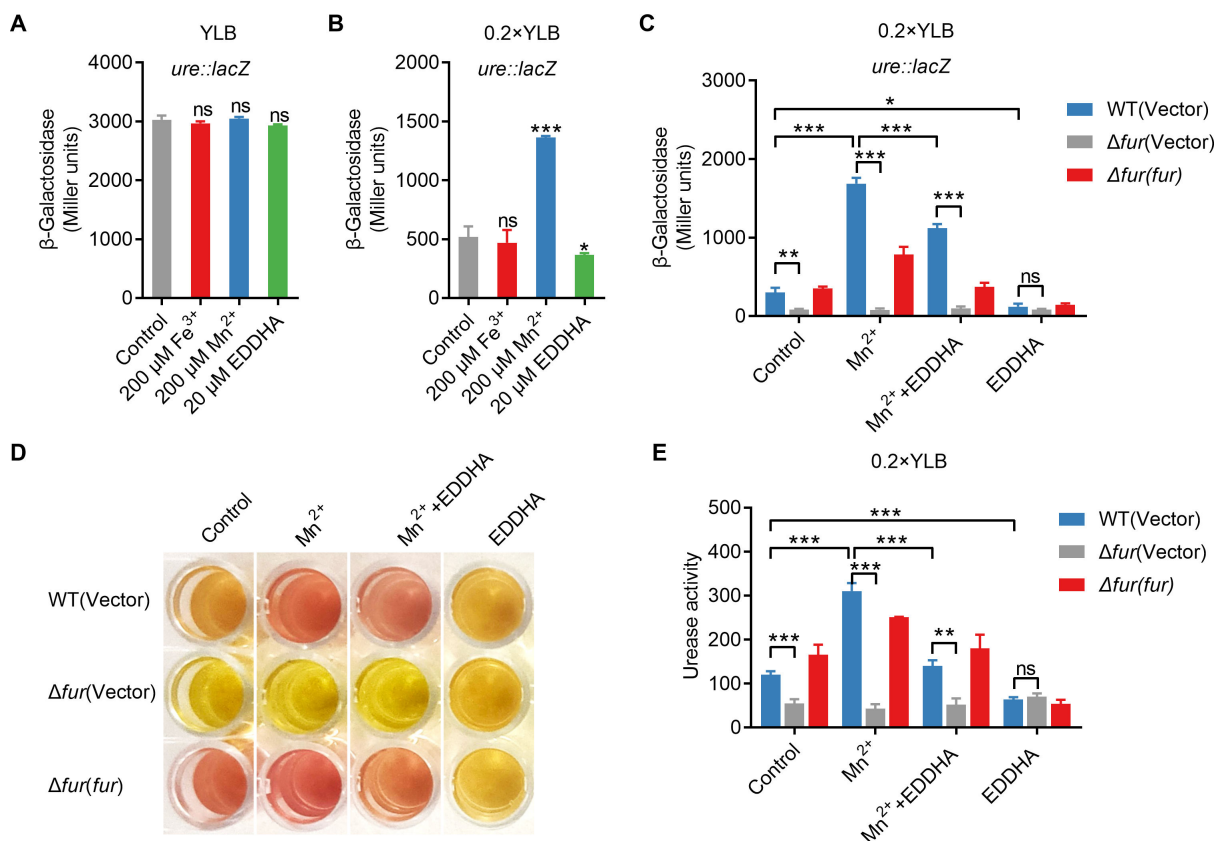


FIG 3 Fur-mediated expression of urease responds to Mn^{2+} under low nutrient conditions. (A) Urease expression is not influenced by Fe^{3+} or Mn^{2+} under relatively rich-nutrient YLB medium. β -galactosidase analysis of urease (*ureABC*) promoter activities was performed in *Yptb* WT strains grown to stationary phase in YLB medium with or without 200 μM Fe^{3+} , 200 μM Mn^{2+} , and 20 μM EDDHA. (B) Urease expression is induced by Mn^{2+} under low nutrient conditions. β -galactosidase analysis of urease (*ureABC*) promoter activities was performed in *Yptb* strains grown to stationary phase in $0.2 \times \text{YLB}$ medium with or without 200 μM Fe^{3+} , 200 μM Mn^{2+} , and 20 μM EDDHA. (C-E) Fur-mediated expression of urease is responsive to Mn^{2+} under low nutrient conditions. The related *Yptb* WT, Δfur , and $\Delta fur(fur)$ strains, either harboring $P_{ureABC}::lacZ$ (C) or not (D and E), were grown to stationary phase in $0.2 \times \text{YLB}$ medium supplemented with 200 μM Mn^{2+} , 200 μM Mn^{2+} + 20 μM EDDHA (Mn^{2+} + EDDHA), or 20 μM EDDHA. The expression of the reporter was measured (C). The urease activity of the indicated bacterial strains was analyzed qualitatively (D) and quantitatively (E). The pH was indicated using phenol red. Urease activity is expressed as micromoles of ammonia produced per minute per milligram of protein. The difference in urease expression in WT, Δfur , and $\Delta fur(fur)$ strains grown to stationary phase in $0.2 \times \text{YLB}$ medium with or without 200 μM Mn^{2+} or 20 μM EDDHA by β -galactosidase analysis of urease promoter activities, qualitative and quantitative urease activity assay. Data represent the mean \pm SD of three biological replicates, each of which was performed with three technical replicates. * $P < 0.05$; ** $P < 0.01$; *** $P < 0.001$; ns, not significant.

Collectively, these results suggest that Fur-mediated expression of urease responds to Mn^{2+} , rather than Fe^{3+} , under low nutrient conditions.

Urease increases the ability of *Yptb* to resist environmental stress and biofilm formation

Urease increases the resistance of many pathogenic bacteria, such as *H. pylori* and *B. abortus*, to an acidic pressure environment (33, 34). To further explore whether urease plays a crucial role in enhancing the survival of *Yptb* under stress conditions, we created the *ureC* (key urease structural gene) deletion mutant and thus determined the viability of the urease mutant after challenge with pH 4.5 EG buffer and 0.5 M NaCl for 40 min. The results showed that the survival rates of the $\Delta ureC$ mutant were significantly more sensitive to acid and osmotic stress than the WT (Fig. 4A and B). Meanwhile, the survival rates of the complemented $\Delta ureC(ureC)$ strain were almost completely restored to the WT levels, supporting a role for urease in combating acid and osmotic stress. Collectively, these data demonstrate that urease contributes to the environmental stress in *Yptb*.

Biofilm is an important strategy adopted by pathogenic bacteria to survive in harsh environments and during host infection (35). *Yptb* is capable of forming biofilm, which contributes to environmental survival and virulence (36). We examined the biofilm-forming capacity of WT and urease biosynthetic mutants using the crystal violet assay. As shown in Fig. 4C and D, the $\Delta ureC$ mutant showed an obvious defect in biofilm formation compared to WT, and the biofilm-formation capacity was restored to WT levels by complementation with *ureC*. Thus, these results indicate that urease plays an important role in resisting adverse stresses and biofilm formation in *Yptb*.

Urease slightly enhances the survival advantage of *Yptb* in infected mice

The urease activity and motility of the pathogen are relevant pathogenic factors for the initial bacterial colonization and survival in the host (37), which led us to further investigate whether urease was involved in the virulence. BALB/c mice were orogastrically infected with the WT and $\Delta ureC$ mutant, respectively, and the survival rate of each group was analyzed. The results showed that infection with the WT resulted in 100% death within 3 weeks of infection, and the lethality rates slightly but substantially decreased in the $\Delta ureC$ mutant infected group (Fig. 5A). Bacterial loads recovered from the feces, cecum, and intestine at 48 h post-infection with *Yptb* strains were then counted. Consistently, mice infected with the $\Delta ureC$ mutant had significantly lower loads

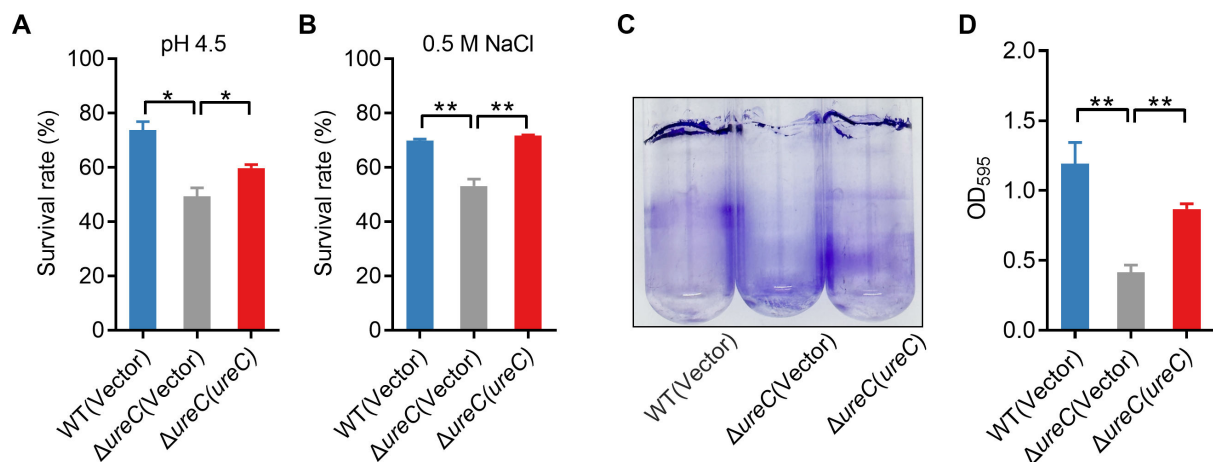


FIG 4 Urease increases the ability of *Yptb* to resist environmental stress and biofilm formation. (A and B) *UreC* is involved in combating acid and osmotic stress. Survival rates of *Yptb* WT, $\Delta ureC$ mutant, and complemented $\Delta ureC(ureC)$ strains after exposure to pH 4.0 (A) or 0.5 M NaCl (B) for 40 min. (C) *UreC* influences the biofilm formation of *Yptb*. The saturated bacterial cultures were diluted 100-fold in a fresh YLB medium. After 3 days of shaking at 150 rpm at 26°C, biofilm formation of the strains was determined by crystal violet staining and quantified using optical density measurement. Data represent the mean \pm SD of three biological replicates, each of which was performed with three technical replicates. * $P < 0.05$; ** $P < 0.01$.

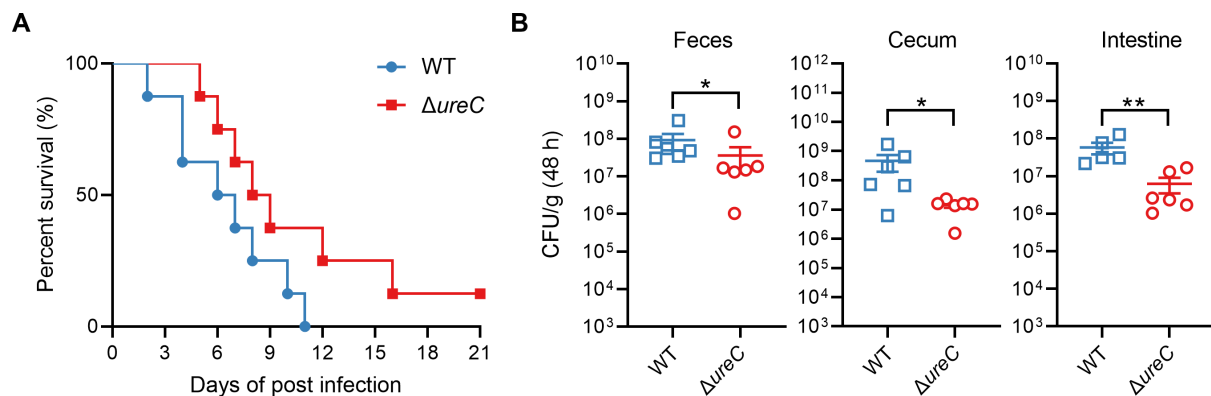


FIG 5 Urease slightly enhances the survival advantage of *Yptb* in infected mice. (A) and (B) *Yptb* WT and $\Delta ureC$ strains grown in YLB were washed twice in sterilized PBS and used for orogastric infection of 6-week-old female BALB/c mice using a ball-tipped feeding needle. For survival assays, 1×10^9 bacteria of each strain were applied to different groups of mice ($n = 9$ /strain), and the survival rate of the mice was determined by monitoring the survival daily for 21 days (A). Enumeration of *Yptb* WT and $\Delta ureC$ strain burdens in the feces, cecum, and intestine of infected BALB/c mice at 48 h post-infection by CFU assays ($n = 6$) (B). Similar results were obtained in three independent experiments, and the data shown are from one representative experiment done in triplicate (A) and (B). The statistical significances were determined by the Mann-Whitney test (B). Data represent the mean \pm SD of three biological replicates, each of which was performed with three technical replicates. The statistical significance was determined by the Mann-Whitney test. * $P < 0.05$; ** $P < 0.01$.

compared to WT-infected mice (Fig. 5B). Taken together, these results suggest that urease contributes to the virulence and survival of *Yptb* in infected mice.

DISCUSSION

Urease is crucial for bacterial colonization in the gastrointestinal tract as it breaks down urea into CO_2 and NH_3 , which helps to neutralize highly acidic environments (6). Studies have shown that urease functions similarly in the acid resistance system of *Yptb* and is regulated by the global factor RovM (2). Recent reports have found that urease activity is regulated by Fur in *E. coli* and *H. pylori* (25, 26). However, it remains unclear whether Fur regulates urease expression in *Yptb*. In this study, we show that urease from *Yptb* is positively regulated by Fur in an Mn^{2+} -dependent manner, which functions to combat acid and osmotic stress and enhance biofilm formation and plays a crucial role in virulence and survival in infected mice.

Bacteria can sense changing external cues, including pH and iron, to control the expression of urease through a number of transcriptional regulators that control their environmental adaptability and virulence (9, 11, 27). For example, *H. pylori* senses the acid signal to induce urease expression through the ArsRS two-component system and the NikR regulatory protein (38). Urease expression in *S. aureus* is regulated by CcpA, Agr, and CodY in response to changes in metabolic flux (9). Our previous studies have shown that *Yptb* senses acid and nutrient conditions to regulate urease expression through OmpR, CsrA, and RovM (2, 5), and here we further investigate the role of Fur in regulating urease expression. Our data show that Fur positively regulates urease expression and activity in *Yptb* (Fig. 1). Although Fur-mediated urease regulation has been studied in other pathogenic bacteria, the regulation mechanisms differ significantly from our findings. For example, Fur positively regulates urease activity in *K. pneumoniae*, probably by controlling intracellular iron and nitrogen concentrations, but not at the transcriptional level (28). In *H. pylori*, mutation of *fur* does not affect urease expression at the transcriptional level or the basal protein level in the medium without nickel. However, nickel, but not iron, manganese, or zinc, induces urease enzyme activity, and the nickel-responsive induction of urease was clearly diminished in *H. pylori* (24). *H. hepaticus* sense iron signal to induce urease expression through Fur (27). Our investigations demonstrate that Fur not only activates the expression of the entire urease gene cluster at the transcriptional level by binding directly to the urease promoter but also positively regulates urease activity in *Yptb* (Fig. 1 and 2). Interestingly, Mn^{2+} , but not

Fe^{3+} , can induce urease expression under low nutrient conditions. Although Fur is an iron-responsive regulator (39), our previous study showed that Fur of *Yptb* is a dual regulator that senses Mn and Fe (21). Further investigations indicate that Fur-mediated expression of *Yptb* urease is responsive to Mn^{2+} under low nutrient conditions, revealing a novel regulatory pathway of the bacterial urease system. While urease contributes to the survival and virulence of *Yptb* in infected mice (Fig. 5), we speculate that *Yptb* may regulate urease levels via Fur after sensing Mn^{2+} concentration upon infection of the host cell, thereby influencing bacterial physiology and pathogenicity.

Urease activity in *Yptb* is subject to complex regulation by different transcriptional regulators, including OmpR, CsrA, RovM, and Fur (2, 5), raising the possibility that urease activity is coordinated by multiple transcriptional regulatory pathways. Each of these regulators responds to different environmental signals and stresses, enabling *Yptb* to fine-tune urease expression in response to changing conditions. For instance, the two-component regulator OmpR positively regulates urease activity in a pH-dependent manner to enhance bacterial acid survival in *Yptb* (5). Under nutrient-rich conditions, RovM and CsrA are suppressed, while the urease activator OmpR is activated, leading to high urease expression. Conversely, under nutrient-limited conditions, OmpR is deactivated, while CsrA is upregulated and RovM is activated, resulting in the repression of urease expression in *Yptb* (2). Furthermore, our data indicate that Fur-activated urease expression is responsive to Mn^{2+} under low nutrient conditions (Fig. 1 and 3). The interconnectivity of these pathways suggests that OmpR, CsrA, RovM, and Fur may form a complex regulatory network to coordinately control urease expression, which is further involved in a variety of important physiological functions. While the specific mechanisms and interconnections of this complex regulatory network in regulating urease in *Yptb* remain unclear, we believe that this intricate regulation reflects the adaptive strategies employed by *Yptb* to optimize urease production and enhance its survival and pathogenicity in response to changing and adverse conditions.

Bacteria have been exposed to a variety of stressful conditions throughout their evolution, including acidity, high osmotic pressure, temperature extremes, and fluctuating nutrient availability. Pathogenic bacteria, in particular, have developed defense strategies including proton pumps, urease, arginine deiminase, sigma factors, and biofilm formation to thrive in acidic environments where they frequently infect hosts (37, 40–43). For example, *S. aureus* utilizes urease to maintain pH balance, protecting itself from reactive oxygen species (ROS) and preserving cell integrity (9). *H. pylori*, a prevalent human pathogen responsible for gastric diseases and potentially gastric cancer, employs ureases to convert urea into CO_2 and NH_3 , adjusting its urease permeability in response to environmental pH changes (44). By contrast, *K. pneumoniae*, which lacks the urease core gene *ureC*, struggles to survive in highly acidic environments at pH 2.5, highlighting the critical role of urease in acid survival (28). Our findings demonstrate that urease enhances *Yptb*'s ability to withstand acid and osmotic stress (Fig. 4), suggesting that urease is a vital mechanism for *Yptb*'s survival under stressful conditions.

The urease system is not only a strategy for obtaining nutrients but also an important tool used by pathogenic bacteria against the host (37, 45). Urease enables *H. pylori* to obtain nutrients and colonize within the host (46, 47). *Cryptococcus neoformans* utilizes urease to cause brain infections in humans (48), where the absence of urease not only inhibits growth but also reduces survival (49). In addition, *Aspergillus fumigatus* spores lacking urease are more susceptible to macrophage-mediated killing (50). Recent research has demonstrated that UreC can interfere with host DNA repair in *Mycobacterium tuberculosis* (51). Therefore, our investigation aimed to assess the effect of urease of the *Yptb* on virulence. Our results showed that mice infected with the ΔureC mutant had a lower mortality rate and bacterial load compared to WT-infected mice. However, there is a different report on whether urease is involved in the virulence of *Yptb* in a previous study (52), probably due to differences in strain characteristics and experimental conditions in these studies. The pYV plasmid, which encodes a key virulence factor,

is present in some but not all *Yptb* strains (53). Riot et al. performed mouse infection experiments using *Yptb* IP2777 (pYV+) WT and $\Delta ureB$, but we used *Yptb* YPIII (pYV-) WT and $\Delta ureC$ to infect mice. Their results have shown that there is no significant difference in Peyer's patches, mesenteric lymph nodes, spleen, and liver between the CFU counts of mice infected with 1×10^8 CFU *Yptb* IP2777 (pYV+) WT or the $\Delta ureB$ mutant strains. Our data indicate that mice infected with 1×10^9 CFU *Yptb* YPIII (pYV-) $\Delta ureC$ mutant had significantly lower loads in the feces, cecum, and intestine compared to WT-infected mice (Fig. 5B), suggesting that urease slightly enhances the survival advantage of *Yptb* YPIII in infected mice. These observations prompt the hypothesis that urease, as a minor virulence factor, may contribute to the virulence and survival of *Yptb* in infected mice in the absence of the key virulence factor encoded by pYV. Moreover, we believe that it is an insufficient argument to conclude that urease is not involved in bacterial virulence only based on the observation that there is no difference in the colonization ability between *Yptb* IP2777 (pYV+) WT and $\Delta ureB$. For example, previous research has demonstrated that the CNF γ toxin does not exert its virulence by enhancing bacterial colonization in mice, but rather by altering the composition of the gut microflora and inducing host inflammatory responses (54). Here, we further analyzed the survival rate of mice after infection with 1×10^9 CFU *Yptb* YPIII (pYV-) WT and $\Delta ureC$ mutant (Fig. 5A), confirming that urease enhances bacterial virulence in a murine model. Thus, the urease produced by *Yptb* YPIII appears to act as a virulence factor. Overall, our results reveal that urease from *Yptb* is directly regulated by Mn²⁺ via Fur, which combats acid and osmotic stress and enhances bacterial virulence and fitness.

MATERIALS AND METHODS

Bacterial strains, plasmid constructions, and growth conditions

The bacterial strains and plasmids used in this study are listed in Table S1. The primers used are detailed in Table S2. *E. coli* strains were grown in Luria-Bertani (LB) broth (1% tryptone, 0.5% yeast extract, and 1% NaCl) with appropriate antibiotics at 37°C, while *Yptb* strains were cultured in Yersinia-Luria-Bertani (YLB) broth (1% tryptone, 0.5% yeast extract, and 0.5% NaCl) or M9 minimal medium (Na₂HPO₄, 6 g L⁻¹; KH₂PO₄, 3 g L⁻¹; NaCl, 0.5 g L⁻¹; NH₄Cl, 1 g L⁻¹; MgSO₄, 2 mM; CaCl₂, 0.1 mM; glucose 0.2%, pH 7.0) at 26°C with appropriate antibiotics when necessary. All chemicals were of Analytical Reagent Grade purity or higher. The *Yptb* YPIII strain was the parent of all derivatives used in this study. To complement the $\Delta ureC$ mutant, we used primers *ureC*-F-BglII/*ureC*-R-Sall to amplify the *ureC* gene from the *Yptb* genomic DNA. The PCR product of *ureC* was then digested with BglII/Sall and inserted into the BamHI/Sall sites of pKT100, resulting in pKT100-*ureC*. Furthermore, the complementary plasmid was introduced into the $\Delta ureC$ mutant by electroporation. The integrity of the insert in all constructs was confirmed by DNA sequencing. Cell growth was monitored by measuring the optical density (OD) at 600 nm. Antibiotics were added at the following concentrations: nalidixic acid, 20 μ g mL⁻¹; kanamycin, 50 μ g mL⁻¹; chloramphenicol, 20 μ g mL⁻¹.

RNA-seq assay

RNA-seq experiment Total RNA was extracted from *Yptb* WT and the Δfur mutant grown in the YLB at 26°C with shaking (220 rpm) to a final OD₆₀₀ of approximately 1.6, using bacteria total RNA isolation kit (TIANGEN, Beijing, China). RNA extraction, library construction, and RNA-seq were commissioned by BGI Genomics (Shenzhen, China). Differential expression analysis was performed using the NOIseq method (Sonia Tarazona 2100). *P*-values were adjusted using the Benjamini and Hochberg method. A corrected *P*-value of 0.05 and log₂(fold change) of 0.8 were set as the threshold for significantly differential expression. Gene Ontology (GO) enrichment analysis of differentially expressed genes was implemented by the Goseq R package, in which gene length bias was corrected. GO terms with corrected *P*-values less than 0.05 were

considered significantly enriched by differentially expressed genes. The data have been deposited under bioProject accession number [PRJNA632467](#).

qRT-PCR

Bacteria cells were harvested during the mid-exponential phase, and RNA was extracted using the RNA prep Pure Cell/Bacteria Kit and treated with RNase-free DNase (TIANGEN, Beijing, China). First-strand cDNA was reverse transcribed from 1 µg of total RNA with the TransScript First-Strand cDNA Synthesis SuperMix (TransGen Biotech, Beijing, China). qRT-PCR was performed in the CFX96 Real-Time PCR Detection System (Bio-Rad, USA) with TransStart Green qPCR SuperMix (TransGen Biotech, Beijing, China). For all primer sets (Table S2), the following cycling parameters were used: 95°C for 30 s followed by 40 cycles of 94°C for 15 s, and 50°C for 30 s. For standardization of results, the relative abundance of 16S rRNA was used as the internal standard. All samples were analyzed in triplicate, and the expression of target genes was calculated as relative fold values using the $2^{-\Delta\Delta CT}$ method. These assays were performed in triplicate at least three times, and error bars represent the standard error of the mean.

β-galactosidase assays

The *lacZ* fusion reporter vector pDM4-*P_{ureABC}::lacZ* was transformed into *E. coli* S17-1λ *pir* and mated with *Yptb* strains as described previously (55). The *lacZ* fusion reporter strains were grown to stationary phase in YLB or 0.2 × YLB at pH 7.0 under 26°C, and β-galactosidase activity was assayed using ONPG (o-Nitrophenyl β-D-galactopyranoside) as the substrate. These assays were performed in triplicate at least three times, and error bars represent standard deviations.

Urease qualitative assay

Phenol red was used as a pH indicator to observe pH changes caused by urease hydrolysis. The qualitative urease tests were carried out according to the methods (29). In summary, the presence of NH₃ results in a pH shift from neutral to alkaline in the medium, using phenol red as the pH indicator. This change is visually indicated by a change in the color of the medium from yellow to pink. After centrifugation at 5,000 g for 10 min, the cells are resuspended in 2 mL of urease test solution (0.5% [wt/vol] NaCl, 0.2% [wt/vol] KH₂PO₄, 0.2% [wt/vol] urea, 0.002% [wt/vol] phenol red), and incubated for 4 h to observe the color of the medium and to determine urease activity.

Urease quantitative assay

Urease activity was quantified by determining the rate of NH₃ production from the hydrolysis of urea (2). Briefly, bacteria were cultured at 26°C and harvested at the late exponential phase. Bacterial cells were washed twice with PBS buffer and then resuspended. Add 5 µL of bacterial suspension to 40 µL of test buffer (0.1% [wt/vol] cetyl dimethyl ammonium bromide [CTAB], 0.6% [wt/vol] NaCl, 100 mM citrate, 5 mM urea, pH 6.0) and incubate with stirring. Add 100 µL of phenol nitroprusside followed by 100 µL alkaline hypochlorite to terminate the reaction. After standing for 30 min at room temperature, the absorbance at 635 nm was measured, and the protein concentration was quantified by the Bradford method using BSA as the standard scale. NH₃ concentration was determined by constructing a standard curve using freshly prepared defined concentrations of NH₄Cl in the same buffer. Urease activity is expressed as micromoles of NH₃ produced per minute per milligram of protein.

Overexpression and purification of recombinant protein

The overexpression and purification of recombinant proteins were conducted according to established methods (56). To express and purify soluble His₆-tagged recombinant proteins, the plasmid pET28a-*fur* was transformed into BL21(DE3). Bacteria were cultured

at 37°C in LB medium to an OD₆₀₀ of 0.5, shifted to 24°C, induced with 0.2 mM IPTG, and then cultivated for an additional 12 h at 24°C. Harvested cells were disrupted by sonication, and proteins were purified with the His-Bind Ni-NTA resin (Novagen, Madison, WI) according to the manufacturer's instructions. Eluted recombinant proteins were dialyzed against buffer (50 mM Tris, 137 mM NaCl, 10% glycerol, pH 7.5) at 4°C. The resulting proteins were stored at -80°C until use. Protein concentrations were determined using the Bradford assay according to the manufacturer's instructions (Bio-Rad, Hercules, CA) with BSA as standard.

Electrophoretic mobility shift assay

The EMSA was performed according to Zuo and colleagues (21). The *P_{ureABC}* fragment was amplified from the *Yptb* YPIII genome using the primers *P_{ureABC}-F* and *P_{ureABC}-R*. Increasing concentrations of purified His₆-Fur (0.12, 0.34, and 1.2 μM) were incubated with 2 ng DNA probes in EMSA buffer (20 mM Tris, pH 7.4, 4 mM MnCl₂, 100 mM NaCl, 1 mM dithiothreitol, and 10% glycerol). After incubation for 30 min at room temperature, the binding reaction mixture was subjected to electrophoresis on a 6% native polyacrylamide gel containing 5% glycerol in 0.5 × TBE (Tris-borate-EDTA) electrophoresis buffer, and the DNA probe was detected using SYBR Green. As a negative control, an irrelevant protein (BSA) was included in the binding assay.

Bacterial survival assays

Mid-exponential phase *Yptb* strains grown in YLB medium were collected, washed, and diluted 50-fold into M9 medium and treated with NaCl (0.5 M) or pH 4.5, respectively, at 26°C for 40 min. After treatment, the cultures were serially diluted and plated onto YLB agar plates, and colonies were counted after 36 h growth at 26°C. Percentage survival was calculated by dividing the number of colony-forming units (CFU) of stressed cells by the number of CFUs of cells without stress. All these assays were performed in triplicate at least three times.

Biofilm formation assay

Biofilm formation was assessed as previously described (57). *Yptb* strains were cultivated in YLB broth and subsequently transferred to 3 mL of M9 medium, shaken at 150 rpm at 26°C. Overnight bacterial cultures were diluted 100-fold in 5 mL of fresh YLB medium, with appropriate antibiotics added when necessary. After vertical incubation for 3 days at 150 rpm and 26°C, the bacterial cultures were removed following OD₆₀₀ measurements, and the test tubes were washed twice with fresh M9. Cells adhering to the test tubes were stained with 0.1% crystal violet for 30 min and then washed twice with M9. The cell-bound dye was eluted in 6 mL of 95% ethanol, and the absorbance of the eluted solution was measured at 590 nm using a microplate reader.

Murine infection assay

The protocol for this study was approved by the Animal Welfare and Research Ethics Committee of Northwest A&F University (Protocol number: XN2023-1004). Six-week-old female BALB/c mice were obtained from SPF Biotechnology Co., Ltd (Beijing, China) and housed in a controlled environment with a temperature of 24 ± 2°C, the humidity of 50 ± 10%, an air flow rate of 35 exchanges per hour, and a light-dark cycle of 12 h each. Mid-exponential phase *Yptb* strains were grown in YLB medium at 26°C, washed twice in sterilized PBS, and used for intragastric or intraperitoneal infection of 6- to 8-week-old female BALB/c mice. For survival assays, 1 × 10⁹ bacteria from each strain were orally gavaged to different groups of mice, and the survival rate was monitored daily for 21 days. To analyze the bacterial load in the feces, fecal samples were collected from individual living mice at 48 h post-infection, weighed, and homogenized in PBS. For the assessment of bacterial load in the cecum and intestine, mice were sacrificed via carbon

dioxide asphyxiation followed by cervical dislocation at 48 h post-infection. The tissues were then weighed and homogenized in PBS, and serial dilutions of the homogenates were plated on YLB plates containing 20 $\mu\text{g mL}^{-1}$ nalidixic acid. The CFUs were counted and reported as CFU per gram of organ or tissue.

Bioinformatics analyses

Sequence alignment and database searches were conducted using the BLAST server on the National Center for Biotechnology Information (NCBI) website (<https://www.ncbi.nlm.nih.gov/>).

Statistical analysis

Experimental data analyzed for significance were analyzed using GraphPad Prism 8 (GraphPad Software, San Diego California USA). The *P* values for mouse survival were calculated using the Log-rank (Mantel-Cox) test. The *P* values for bacterial CFU in mouse tissues were calculated using the Mann-Whitney test (I). Statistical analyses for the rest of the assays were performed using unpaired two-tailed Student's *t*-test. Error bars represent \pm SD. **P* < 0.05; ***P* < 0.01; ****P* < 0.001.

ACKNOWLEDGMENTS

This work was supported by grants from the National Natural Science Foundation of China (Grants 32470039 and 32100149 to L.Z., 32330004 to X.S., 32470197 and 32100034 to C.L.) and the Young Talent Support Program of Shaanxi Province University (Grant No. 20220206 to L.Z.).

J.W., P.F., and L.Z. designed the research. J.W., P.F., X.H., and Y.L. performed the experimental work. J.W., P.F., X.H., Y.L., Y.Z., Z.W., Y.W., Y.Y., C.L., and L.Z. analyzed the data. L.Z., J.W., and P.F. drafted the manuscript. X.S. revised the manuscript. The author(s) read and approved the final manuscript.

AUTHOR AFFILIATION

¹State Key Laboratory for Crop Stress Resistance and High-Efficiency Production, Shaanxi Key Laboratory of Agricultural and Environmental Microbiology, College of Life Sciences, Northwest A&F University, Yangling, Shaanxi, China

AUTHOR ORCIDs

Peishuai Fu  <http://orcid.org/0009-0007-3408-5013>
 Yao Wang  <https://orcid.org/0000-0002-7149-4234>
 Yantao Yang  <https://orcid.org/0000-0002-2489-7639>
 Changfu Li  <https://orcid.org/0000-0001-7791-6111>
 Xihui Shen  <http://orcid.org/0000-0001-6867-8887>
 Lingfang Zhu  <http://orcid.org/0000-0002-1116-9296>

FUNDING

Funder	Grant(s)	Author(s)
MOST National Natural Science Foundation of China (NSFC)	32470039, 32100149	Lingfang Zhu
MOST National Natural Science Foundation of China (NSFC)	32330004	Xihui Shen
MOST National Natural Science Foundation of China (NSFC)	32470197, 32100034	Changfu Li
Young Talent Support Program of Shaanxi Province University	20220206	Lingfang Zhu

AUTHOR CONTRIBUTIONS

Junyang Wang, Conceptualization, Data curation, Formal analysis, Resources, Writing – original draft | Peishuai Fu, Conceptualization, Data curation, Formal analysis, Writing – original draft | Xinquan He, Data curation, Formal analysis | Yuqi Liu, Data curation, Formal analysis | Yuxin Zuo, Data curation, Formal analysis | Zhiyan Wei, Data curation, Formal analysis | Yao Wang, Data curation, Formal analysis | Yantao Yang, Data curation, Formal analysis | Changfu Li, Data curation, Formal analysis | Xihui Shen, Funding acquisition, Writing – review and editing | Lingfang Zhu, Conceptualization, Data curation, Formal analysis, Investigation, Resources, Writing – original draft

DATA AVAILABILITY

All data sets generated for this study are included in the article/Supplementary Information.

ADDITIONAL FILES

The following material is available [online](#).

Supplemental Material

Supplemental material (Spectrum02756-24-s0001.docx). Fig. S1; Tables S1 and S2.

REFERENCES

- Galindo CL, Rosenzweig JA, Kirtley ML, Chopra AK. 2011. Pathogenesis of *Y. enterocolitica* and *Y. pseudotuberculosis* in human yersiniosis. *J Pathog* 2011:182051. <https://doi.org/10.4061/2011/182051>
- Dai Q, Xu L, Xiao L, Zhu K, Song Y, Li C, Zhu L, Shen X, Wang Y. 2018. RovM and CsrA negatively regulate urease expression in *Yersinia pseudotuberculosis*. *Front Microbiol* 9:348. <https://doi.org/10.3389/fmicb.2018.00348>
- Aquino P, Honda B, Jaini S, Lyubetskaya A, Hosur K, Chiu JG, Ekladios I, Hu D, Jin L, Sayeg MK, et al. 2017. Coordinated regulation of acid resistance in *Escherichia coli*. *BMC Syst Biol* 11:1. <https://doi.org/10.1186/s12918-016-0376-y>
- Song Y, Xiao X, Li C, Wang T, Zhao R, Zhang W, Zhang L, Wang Y, Shen X. 2015. The dual transcriptional regulator RovM regulates the expression of AR3- and T6SS4-dependent acid survival systems in response to nutritional status in *Yersinia pseudotuberculosis*. *Environ Microbiol* 17:4631–4645. <https://doi.org/10.1111/1462-2920.12996>
- Hu Y, Lu P, Wang Y, Ding L, Atkinson S, Chen S. 2009. OmpR positively regulates urease expression to enhance acid survival of *Yersinia pseudotuberculosis*. *Microbiology (Reading, Engl)* 155:2522–2531. <https://doi.org/10.1099/mic.0.028381-0>
- Kappaun K, Piovesan AR, Carlini CR, Ligabue-Braun R. 2018. Ureases: historical aspects, catalytic, and non-catalytic properties - a review. *J Adv Res* 13:3–17. <https://doi.org/10.1016/j.jare.2018.05.010>
- Mora D, Maguin E, Masiero M, Parini C, Ricci G, Manachini PL, Daffonchio D. 2004. Characterization of urease genes cluster of *Streptococcus thermophilus*. *J Appl Microbiol* 96:209–219. <https://doi.org/10.1046/j.1365-2672.2003.02148.x>
- Koper TE, El-Sheikh AF, Norton JM, Klotz MG. 2004. Urease-encoding genes in ammonia-oxidizing bacteria. *Appl Environ Microbiol* 70:2342–2348. <https://doi.org/10.1128/AEM.70.4.2342-2348.2004>
- Zhou C, Bhinderwala F, Lehman MK, Thomas VC, Chaudhari SS, Yamada KJ, Foster KW, Powers R, Kielian T, Fey PD. 2019. Urease is an essential component of the acid response network of *Staphylococcus aureus* and is required for a persistent murine kidney infection. *PLoS Pathog* 15:e1007538. <https://doi.org/10.1371/journal.ppat.1007538>
- Nieckarz M, Kaczor P, Jaworska K, Raczowska A, Brzostek K. 2020. Urease expression in pathogenic *Yersinia enterocolitica* strains of bio-serotypes 2/O:9 and 1B/O:8 is differentially regulated by the OmpR regulator. *Front Microbiol* 11:607. <https://doi.org/10.3389/fmicb.2020.00607>
- Xia X. 2022. Multiple regulatory mechanisms for pH homeostasis in the gastric pathogen, *Helicobacter pylori*. *Adv Genet* 109:39–69. <https://doi.org/10.1016/bs.adgen.2022.07.001>
- Righetto RD, Anton L, Adaixo R, Jakob RP, Zivanov J, Mahi MA, Ringler P, Schwede T, Maier T, Stahlberg H. 2020. High-resolution cryo-EM structure of urease from the pathogen *Yersinia enterocolitica*. *Nat Commun* 11:5101. <https://doi.org/10.1038/s41467-020-18870-2>
- De Koning-Ward TF, Robins-Browne RM. 1995. Contribution of urease to acid tolerance in *Yersinia enterocolitica*. *Infect Immun* 63:3790–3795. <https://doi.org/10.1128/iai.63.10.3790-3795.1995>
- Collins CM, D'Orazio SE. 1993. Bacterial ureases: structure, regulation of expression and role in pathogenesis. *Mol Microbiol* 9:907–913. <https://doi.org/10.1111/j.1365-2958.1993.tb01220.x>
- Mobley HL, Hausinger RP. 1989. Microbial ureases: significance, regulation, and molecular characterization. *Microbiol Rev* 53:85–108. <https://doi.org/10.1128/mr.53.1.85-108.1989>
- Pflock M, Kennard S, Finsterer N, Beier D. 2006. Acid-responsive gene regulation in the human pathogen *Helicobacter pylori*. *J Biotechnol* 126:52–60. <https://doi.org/10.1016/j.jbiotec.2006.03.045>
- Benoit SL, Maier RJ. 2011. UreA (HP0868) is a nickel-binding protein that modulates urease activity in *Helicobacter pylori*. *MBio* 2:e00039-11. <https://doi.org/10.1128/mBio.00039-11>
- Coker C, Bakare OO, Mobley HL. 2000. H-NS is a repressor of the *Proteus mirabilis* urease transcriptional activator gene *ureR*. *J Bacteriol* 182:2649–2653. <https://doi.org/10.1128/JB.182.9.2649-2653.2000>
- Fillat MF. 2014. The Fur (ferric uptake regulator) superfamily: diversity and versatility of key transcriptional regulators. *Arch Biochem Biophys* 546:41–52. <https://doi.org/10.1016/j.abb.2014.01.029>
- Valenzuela M, Albar JP, Paradelo A, Toledo H. 2011. *Helicobacter pylori* exhibits a Fur-dependent acid tolerance response. *Helicobacter* 16:189–199. <https://doi.org/10.1111/j.1523-5378.2011.00824.x>
- Zuo Y, Li C, Yu D, Wang K, Liu Y, Wei Z, Yang Y, Wang Y, Shen X, Zhu L. 2023. A Fur-regulated type VI secretion system contributes to oxidative stress resistance and virulence in *Yersinia pseudotuberculosis*. *Stress Biol* 3:2. <https://doi.org/10.1007/s44154-022-00081-y>
- Li C, Pan D, Li M, Wang Y, Song L, Yu D, Zuo Y, Wang K, Liu Y, Wei Z, Zhu L, Shen X. 2021. Aerobactin-mediated iron acquisition enhances biofilm formation, oxidative stress resistance, and virulence of *Yersinia pseudotuberculosis*. *Front Microbiol* 12:699913. <https://doi.org/10.3389/fmicb.2021.699913>
- Zhu L, Xu L, Wang C, Li C, Li M, Liu Q, Wang X, Yang W, Pan D, Hu L, Yang Y, Lu Z, Wang Y, Zhou D, Jiang Z, Shen X. 2021. T6SS translocates a micropeptide to suppress STING-mediated innate immunity by sequestering manganese. *Proc Natl Acad Sci USA* 118. <https://doi.org/10.1073/pnas.2103526118>

24. van Vliet AH, Kuipers EJ, Waidner B, Davies BJ, de Vries N, Penn CW, Vandenbroucke-Grauls CM, Kist M, Bereswill S, Kusters JG. 2001. Nickel-responsive induction of urease expression in *Helicobacter pylori* is mediated at the transcriptional level. *Infect Immun* 69:4891–4897. <https://doi.org/10.1128/IAI.69.8.4891-4897.2001>
25. Lee JS, Choe YH, Lee JH, Lee HJ, Lee JH, Choi YO. 2010. *Helicobacter pylori* urease activity is influenced by ferric uptake regulator. *Yonsei Med J* 51:39–44. <https://doi.org/10.3349/ymj.2010.51.1.39>
26. Heimer SR, Welch RA, Perna NT, Pósfai G, Evans PS, Kaper JB, Blattner FR, Mobley HLT. 2002. Urease of enterohemorrhagic *Escherichia coli*: evidence for regulation by Fur and a trans-acting factor. *Infect Immun* 70:1027–1031. <https://doi.org/10.1128/IAI.70.2.1027-1031.2002>
27. Belzer C, van Schendel BAM, Kuipers EJ, Kusters JG, van Vliet AHM. 2007. Iron-responsive repression of urease expression in *Helicobacter hepaticus* is mediated by the transcriptional regulator Fur. *Infect Immun* 75:745–752. <https://doi.org/10.1128/IAI.01163-06>
28. Lin WF, Hu RY, Chang HY, Lin FY, Kuo CH, Su LH, Peng HL. 2022. The role of urease in the acid stress response and fimbriae expression in *Klebsiella pneumoniae* CG43. *J Microbiol Immunol Infect* 55:620–633. <https://doi.org/10.1016/j.jmii.2022.02.002>
29. Young GM, Amid D, Miller VL. 1996. A bifunctional urease enhances survival of pathogenic *Yersinia enterocolitica* and *Morganella morganii* at low pH. *J Bacteriol* 178:6487–6495. <https://doi.org/10.1128/jb.178.22.6487-6495.1996>
30. Grifantini R, Sebastian S, Frigimelica E, Draghi M, Bartolini E, Muzzi A, Rappuoli R, Grandi G, Genco CA. 2003. Identification of iron-activated and -repressed Fur-dependent genes by transcriptome analysis of *Neisseria meningitidis* group B. *Proc Natl Acad Sci U S A* 100:9542–9547. <https://doi.org/10.1073/pnas.1033001100>
31. Troxell B, Hassan HM. 2013. Transcriptional regulation by ferric uptake regulator (Fur) in pathogenic bacteria. *Front Cell Infect Microbiol* 3:59. <https://doi.org/10.3389/fcimb.2013.00059>
32. Kang SM, Kang HS, Chung WH, Kang KT, Kim DH. 2024. Structural perspectives on metal dependent roles of ferric uptake regulator (Fur). *Biomolecules* 14:981. <https://doi.org/10.3390/biom14080981>
33. Stingl K, Altendorf K, Bakker EP. 2002. Acid survival of *Helicobacter pylori*: how does urease activity trigger cytoplasmic pH homeostasis? *Trends Microbiol* 10:70–74. [https://doi.org/10.1016/s0966-842x\(01\)02287-9](https://doi.org/10.1016/s0966-842x(01)02287-9)
34. Sangari FJ, Seoane A, Rodríguez MC, Agüero J, García Lobo JM. 2007. Characterization of the urease operon of *Brucella abortus* and assessment of its role in virulence of the bacterium. *Infect Immun* 75:774–780. <https://doi.org/10.1128/IAI.01244-06>
35. Donlan RM, Costerton JW. 2002. Biofilms: survival mechanisms of clinically relevant microorganisms. *Clin Microbiol Rev* 15:167–193. <https://doi.org/10.1128/CMR.15.2.167-193.2002>
36. Schachterle JK, Stewart RM, Schachterle MB, Calder JT, Kang H, Prince JT, Erickson DL. 2018. *Yersinia pseudotuberculosis* BarA-UvrY two-component regulatory system represses biofilms via CsrB. *Front Cell Infect Microbiol* 8:323. <https://doi.org/10.3389/fcimb.2018.00323>
37. Mora D, Arioli S. 2014. Microbial urease in health and disease. *PLoS Pathog* 10:e1004472. <https://doi.org/10.1371/journal.ppat.1004472>
38. Pflock M, Kennard S, Delany I, Scarlato V, Beier D. 2005. Acid-induced activation of the urease promoters is mediated directly by the ArsRS two-component system of *Helicobacter pylori*. *Infect Immun* 73:6437–6445. <https://doi.org/10.1128/IAI.73.10.6437-6445.2005>
39. Beauchene NA, Myers KS, Chung D, Park DM, Weisnicht AM, Keleş S, Kiley PJ. 2015. Impact of anaerobiosis on expression of the iron-responsive Fur and RyhB regulons. *MBio* 6:e01947-15. <https://doi.org/10.1128/mbio.01947-15>
40. Lee C, Mariani KJ. 2013. Characterization of the nucleoid-associated protein YejK. *J Biol Chem* 288:31503–31516. <https://doi.org/10.1074/jbc.M113.494237>
41. Xiong L, Teng JLL, Botelho MG, Lo RC, Lau SKP, Woo PCY. 2016. Arginine metabolism in bacterial pathogenesis and cancer therapy. *Int J Mol Sci* 17:363. <https://doi.org/10.3390/ijms17030363>
42. Fang FC, Libby SJ, Buchmeier NA, Loewen PC, Switala J, Harwood J, Guiney DG. 1992. The alternative sigma factor KatF (RpoS) regulates *Salmonella* virulence. *Proc Natl Acad Sci U S A* 89:11978–11982. <https://doi.org/10.1073/pnas.89.24.11978>
43. Flemming HC, Wingender J, Szewzyk U, Steinberg P, Rice SA, Kjelleberg S. 2016. Biofilms: an emergent form of bacterial life. *Nat Rev Microbiol* 14:563–575. <https://doi.org/10.1038/nrmicro.2016.94>
44. Zilberman Y, Sonkusale SR. 2015. Microfluidic optoelectronic sensor for salivary diagnostics of stomach cancer. *Biosens Bioelectron* 67:465–471. <https://doi.org/10.1016/j.bios.2014.09.006>
45. Konieczna I, Zarnowiec P, Kwinkowski M, Kolesinska B, Fraczyk J, Kaminski Z, Kaca W. 2012. Bacterial urease and its role in long-lasting human diseases. *Curr Protein Pept Sci* 13:789–806. <https://doi.org/10.2174/138920312804871094>
46. Eaton KA, Brooks CL, Morgan DR, Krakowka S. 1991. Essential role of urease in pathogenesis of gastritis induced by *Helicobacter pylori* in gnotobiotic piglets. *Infect Immun* 59:2470–2475. <https://doi.org/10.1128/iai.59.7.2470-2475.1991>
47. Huang JY, Sweeney EG, Sigal M, Zhang HC, Remington SJ, Cantrell MA, Kuo CJ, Guillemin K, Amieva MR. 2015. Chemodetection and destruction of host urea allows *Helicobacter pylori* to locate the epithelium. *Cell Host Microbe* 18:147–156. <https://doi.org/10.1016/j.chom.2015.07.002>
48. Singh A, Panting RJ, Varma A, Saijo T, Waldron KJ, Jong A, Ngamskulrungrat P, Chang YC, Rutherford JC, Kwon-Chung KJ. 2013. Factors required for activation of urease as a virulence determinant in *Cryptococcus neoformans*. *MBio* 4:e00220-13. <https://doi.org/10.1128/mBio.00220-13>
49. Toplis B, Bosch C, Schwartz IS, Kenyon C, Boekhout T, Perfect JR, Botha A. 2020. The virulence factor urease and its unexplored role in the metabolism of *Cryptococcus neoformans*. *FEMS Yeast Res* 20:foaa031. <https://doi.org/10.1093/femsyr/foaa031>
50. Xiong Z, Zhang N, Xu L, Deng Z, Limwachiranon J, Guo Y, Han Y, Yang W, Scharf DH. 2023. Urease of *Aspergillus fumigatus* is required for survival in macrophages and virulence. *Microbiol Spectr* 11:e0350822. <https://doi.org/10.1128/spectrum.03508-22>
51. Liu S, Guan L, Peng C, Cheng Y, Cheng H, Wang F, Ma M, Zheng R, Ji Z, Cui P, Ren Y, Li L, Shi C, Wang J, Huang X, Cai X, Qu D, Zhang H, Mao Z, Liu H, Wang P, Sha W, Yang H, Wang L, Ge B. 2023. *Mycobacterium tuberculosis* suppresses host DNA repair to boost its intracellular survival. *Cell Host Microbe* 31:1820–1836. <https://doi.org/10.1016/j.chom.2023.09.010>
52. Riot B, Berche P, Simonet M. 1997. Urease is not involved in the virulence of *Yersinia pseudotuberculosis* in mice. *Infect Immun* 65:1985–1990. <https://doi.org/10.1128/iai.65.5.1985-1990.1997>
53. Gkouletsos T, Patas K, Lambrinidis G, Neubauer H, Sprague LD, Ioannidis A, Chatzipanagiotou S. 2019. Antimicrobial resistance of *Yersinia enterocolitica* and presence of plasmid pYV virulence genes in human and animal isolates. *New Microbes New Infect* 32:100604. <https://doi.org/10.1016/j.nmni.2019.100604>
54. Heine W, Beckstette M, Heroven AK, Thiemann S, Heise U, Nuss AM, Pisano F, Strowig T, Dersch P. 2018. Loss of CNF γ toxin-induced inflammation drives *Yersinia pseudotuberculosis* into persistency. *PLoS Pathog* 14:e1006858. <https://doi.org/10.1371/journal.ppat.1006858>
55. Wang D, Zhu L, Zhen X, Yang D, Li C, Chen Y, Wang H, Qu Y, Liu X, Yin Y, Gu H, Xu L, Wan C, Wang Y, Ouyang S, Shen X. 2022. A secreted effector with a dual role as a toxin and as a transcriptional factor. *Nat Commun* 13:7779. <https://doi.org/10.1038/s41467-022-35522-9>
56. Li C, Zhu L, Wang D, Wei Z, Hao X, Wang Z, Li T, Zhang L, Lu Z, Long M, Wang Y, Wei G, Shen X. 2022. T6SS secretes an LPS-binding effector to recruit OMVs for exploitative competition and horizontal gene transfer. *ISME J* 16:500–510. <https://doi.org/10.1038/s41396-021-01093-8>
57. Yang Y, Pan D, Tang Y, Li J, Zhu K, Yu Z, Zhu L, Wang Y, Chen P, Li C. 2022. H3-T6SS of *Pseudomonas aeruginosa* PA14 contributes to environmental adaptation via secretion of a biofilm-promoting effector. *Stress Biol* 2:55. <https://doi.org/10.1007/s44154-022-00078-7>